2009

A New Technique For Timing The Double Pulsar System

P. C. C. Freire

N. Wex

M. Kramer

D. R. Lorimer

M. A. McLaughlin

See next page for additional authors

Mon. Not. R. Astron. Soc. **396,** 1764–1770 (2009) doi:10.1111/j.1365-2966.2009.14862.x

A new technique for timing the double pulsar system

P. C. C. Freire,[1,2⋆] N. Wex,[3] M. Kramer,[3,4] D. R. Lorimer,[2] M. A. McLaughlin,[2] I. H. Stairs,[5,6] R. Rosen[7] and A. G. Lyne[4]

[1]*Arecibo Observatory, HC3 Box 53995, Arecibo, PR 00612, USA*
[2]*Department of Physics, West Virginia University, PO Box 6315 Morgantown, WV 26506-6315, USA*
[3]*Max-Planck Institut für Radioastronomie, Auf dem Hügel 69, 53121 Bonn, Germany*
[4]*University of Manchester, Jodrell Bank Centre for Astrophysics, Alan-Turing Building, Oxford Road, Manchester, M13 9PL*
[5]*University of British Columbia, 6224 Agricultural Road Vancouver, BC V6T 1Z1 Canada*
[6]*ATNF, PO Box 76, Epping NSW 1710, Australia*
[7]*NRAO, Green Bank, WV 24944-0002, USA*

Accepted 2009 April 2. Received 2009 March 24; in original form 2009 February 3

ABSTRACT

In 2004, McLaughlin et al. discovered a phenomenon in the radio emission of PSR J0737−3039B (B) that resembles drifting subpulses. The repeat rate of the subpulses is equal to the spin frequency of PSR J0737−3039A (A); this led to the suggestion that they are caused by incidence upon B's magnetosphere of electromagnetic radiation from A. Here, we describe a geometrical model which predicts the delay of B's subpulses relative to A's radio pulses. We show that measuring these delays is equivalent to tracking A's rotation from the point of view of a hypothetical observer located near B. This has three main astrophysical applications: (i) to determine the sense of rotation of A relative to its orbital plane, (ii) to estimate where in B's magnetosphere the radio subpulses are modulated and (iii) to provide an independent estimate of the mass ratio of A and B. The latter might improve existing tests of gravitational theories using this system.

Key words: binaries: general – pulsars: general – pulsars: individual: PSR J0737−3039A – pulsars: individual: PSR J0737−3039B.

1 INTRODUCTION

The discovery of the double pulsar system PSR J0737−3039 (Burgay et al. 2003; Lyne et al. 2004) has led to important advances in the study of radio pulsars and their associated phenomenology. The independent determination of the orbit of both neutron stars, and the recent measurement of five post-Keplerian parameters from the timing of PSR J0737−3039A (henceforth A) (Kramer et al. 2006) and a sixth one from eclipse observations of A (Breton et al. 2008) have made this the most overconstrained system known, allowing five tests of general relativity.

PSR J0737−3039B (henceforth B) has many unique features. It emits pulsed radio waves during most of the orbit, but it becomes much brighter at two distinct orbital phases (Lyne et al. 2004). Furthermore, its pulse profile changes strongly with orbital phase and with time (Burgay et al. 2005). Though instructive in other ways, this behaviour has made it difficult to measure times of arrival accurately and obtain a precise estimate of the semimajor axis of the orbit of B, limiting the precision of our knowledge of the pulsar mass ratio $R = m_A/m_B$ and the precision of some of the tests of general relativity in this system (see e.g. Kramer & Stairs 2008 for a recent review).

This paper is motivated by another unique feature of B: for certain orbital phases, its radio emission is clearly modulated by electromagnetic emission from A (McLaughlin et al. 2004); the phenomenon superficially resembles drifting subpulses (e.g. Lorimer & Kramer 2005). In this work, we discuss the *timing* of this phenomenon. In Section 2, we present a theoretical calculation of the delay in the arrival at the Earth of the subpulses of B relative to the radio pulses of A responsible for the drift. We name this simply the 'response delay'. In Section 3, we discuss how we can compare the predicted and measured response delays. In Section 4, we highlight the astrophysical knowledge that can be gained from the timing of the response delays.

2 CALCULATING RESPONSE DELAYS

2.1 Time between emission of A's radio pulse and B's response

The time between the emission of A's radio pulse and B's response can be divided in three parts, which we discuss below.

⋆E-mail: pfreire@naic.edu

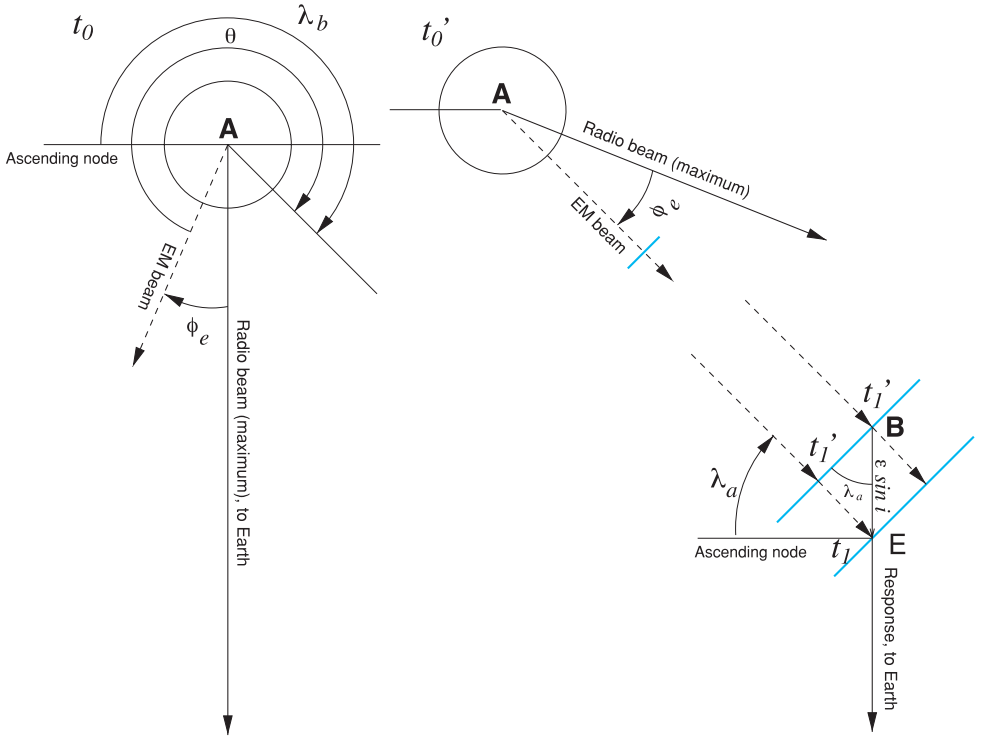

Figure 1. Sequence of events in A, looking down the pulsar's spin axis. We assume that the plane of the drawing is the orbital plane. Left: at t_0, the radio beam is pointing at the Earth (outside of the orbital plane), producing a maximum of radio emission. At this time, A's EM beam is not necessarily pointing at B. Centre top: at t_0', A is emitting the EM signal that will produce the response. Locally, the wavefront (light line) is a plane perpendicular to the direction of propagation of the EM signal. Between t_0 and t_0', A rotated by $\theta = \lambda_b + \pi/2 - \phi_e$ if the pulsar is rotating in the same sense of the orbit (clockwise here), or $\theta = 2\pi - (\lambda_b + \pi/2 - \phi_e)$ if the pulsar is rotating in the opposite sense of the orbit. Right bottom: at time t_1', the EM wavefront arrives at B's position. Soon after that, at time t_1, the wavefront arrives at point E, where the Earth-bound radio emission of B originates. This is located at a fixed distance ϵ from B on that pulsar's line-of-sight to Earth, it is at a small distance from the orbital plane $\epsilon \cos i$ (see text). The arrival of the wavefront at point E at time t_1 produces the response in B's emission, which then follows to Earth. λ_a is the longitude of A as seen from E at t_1; so $\lambda_b = \lambda_a + \pi$ is the longitude at which A's EM beam transmits towards B.

(i) The subpulses of B are spaced by 22.7 ms, which is the same as the spin period of A (McLaughlin et al. 2004). Therefore, we can think of the maximum intensity of the subpulses of B (the 'response') as being caused by the impact upon B's radio emitting region of a co-rotating beam of electromagnetic radiation from A. We henceforth refer to this as the EM beam. Since the EM beam is not necessarily aligned in rotational phase with A's radio beam, as shown in Fig. 1, we introduce a phase offset ϕ_e between the two beams. We define A's zero longitude to be the point where the radio emission towards the Earth reaches maximum intensity. As we show later, one of the applications of our model would be the direct determination of ϕ_e.

One of the simplifying assumptions in Fig. 1 is that the spin axis of A is perpendicular to the orbital plane. This has been suggested (Manchester et al. 2005) as the most plausible explanation for the lack of change in the pulse profile of A; Ferdman (2008) set an upper limit of about 14° for the misalignment between the orbital angular momentum and the spin of A. We henceforth assume that the spin axis of A is indeed perpendicular to the orbital plane. It is not known whether A rotates in the same sense as the orbit or in the opposite sense, but kinematic considerations (Bailes 1988) make the former more likely. We discuss this issue further in Sections 3 and 4.

In Fig. 1, at time t_0 we see A's radio beam pointing at the Earth, causing the radio emission to reach a maximum. At time t_0', the EM beam is pointing at a direction λ_b, where it emits the signal that will later cause B's response.[1] Between the two events, A has rotated by an angle $\theta = \pm(\lambda_a - \pi/2 - \phi_e)$ where $\lambda_a = \lambda_b - \pi$ is the longitude of A as seen from the location and time where the EM signal modulated the radio pulse of B (point E at time t_1; see Fig. 1). The positive sign corresponds to a clockwise rotation of A as shown in Fig. 1, i.e. in the same sense of the orbit. The time between the two events is given by

$$t_0' - t_0 = P_{\rm A}\frac{\theta}{2\pi}, \tag{1}$$

where $P_{\rm A}$ is the spin period of A.

(ii) After t_0', the EM pulse of A travels towards B; at time t_1', it gets to B's exact position. The distance between these two events is $r_{\rm AB}(\lambda_a)$, this is calculated in Section 2.3. In the assumption above (that signal travels at the speed of light), we have

$$t_1' - t_0' = \frac{r_{\rm AB}(\lambda_a)}{c}. \tag{2}$$

(iii) What happens near B is less certain. The simplest assumption is that the EM signal is able to travel through B's magnetosphere

[1] Lower-case subscripts refer to λ computed for the emission-reception-Earth triangle, while uppercase subscripts refer to lambda computed for a line through the centre of mass of the binary system, O. Here, we have neglected aberration effects and the small angle between AB and AE, as the corresponding time delays are below the accuracy relevant for this paper.

at the speed of light (this is possible, e.g. if the EM signal consists of high-energy photons) and modulates B's Earth-bound radio emission at the point where it is being generated; we designate this as 'E'. We must keep in mind that this simplified assumption is not the only possible case: (i) the modulation could occur after B's radio signal is produced, i.e. somewhere between point E and the Earth and (ii) more generally, the chain of events from the emission of the EM signal at A (t'_0) to the modulation of the radio signal of B (t_1) might not lie along a single null geodesic. For the time being, we will quantify the simplest case only (see Fig. 1).

Since E is where the Earth-bound radio emission is being generated, we assume it is the point of the radio-emitting region of B's magnetosphere that is in the line-of-sight from B to Earth. This only happens when B's radio pulse is 'on'. For most of B's rotational cycle, when its pulse is 'off', no part of its radio-emitting region is pointing at Earth, and no response is detected.

In our simplified model, we assume that the distance of E to B is a constant ϵ as a function of B's spin phase. Therefore, in the reference frame of the orbital plane (with axes along the line of nodes, perpendicular to the line of nodes and perpendicular to the orbital plane), E is located at fixed coordinates $(0, \epsilon \sin i, \epsilon \cos i)$ relative to B, where i is the orbital inclination of the system (see Fig. 1).

At t'_1, the EM wavefront from A reaches B. A small amount of time later, at t_1, the same wavefront reaches E and produces the response. From that figure, we can see that

$$t_1 - t'_1 = \frac{\epsilon}{c} \sin\lambda_a \sin i. \tag{3}$$

Between t'_1 and t_1, the orbital motion of B will make E move by a small amount relative to the centre of the binary. This will affect the arrival time at E. We note, however, that for slow pulsars ϵ/c is expected to be of the order of 1 ms (Blaskiewicz, Cordes & Wasserman 1991). Assuming this is true, a detailed calculation of the $O(\epsilon c^{-2})$ Doppler correction due to B's (and E's) motion shows that this term is smaller than 1 μs. Since the rms timing precision of A is about 10 μs, and the timing precision for B's response is likely to be worse, we will ignore all terms with magnitude <10 μs.

For the total time difference, we obtain

$$\begin{aligned} t_1 - t_0 &\equiv (t_1 - t'_1) + (t'_1 - t'_0) + (t'_0 - t_0) \\ &= \frac{\epsilon}{c} \sin\lambda_a \sin i + \frac{r_{\rm AB}(\lambda_a)}{c} + P_{\rm A}\frac{\theta}{2\pi} + O\left(\epsilon c^{-2}\right), \end{aligned} \tag{4}$$

which should be valid in any inertial reference frame using the orbital parameters as measured in that frame.

2.2 Response delay

We now calculate the delay between the reception at the SSB of A's radio pulses and B's responses, $\Delta(\lambda_a)$. To do this, we will start by adding to $t_1 - t_0$ the difference in the ranges[2] at which these events occur, $z_1 - z_0$ divided by c; this is the so-called 'Rømer delay'.

As in the case of $t_1 - t_0$ (equation 4), $z_1 - z_0$ can also be described as the sum of three terms, $(z_1 - z'_1) + (z'_1 - z'_0) + (z'_0 - z_0)$:

[2] We use the term 'range' to indicate the distance of a given event from the centre of mass of the binary projected along the direction to the SSB *as seen at the SSB*.

(i) The difference in range between the events at t_0 and t'_0 is given by

$$z'_0 - z_0 = (t'_0 - t_0) v_{l,A} = P_{\rm A}\frac{\theta}{2\pi} v_{l,A}, \tag{5}$$

where $v_{l,A}$ is the velocity of A relative to the centre of mass, projected along the line-of-sight to Earth (Section 2.3).

(ii) In the lower diagram of Fig. 2, we see that the difference in range between the events happening at t'_1 and t'_0 is given by

$$z'_1 - z'_0 = -r_{\rm AB}(\lambda_a) \sin\lambda_a \sin i. \tag{6}$$

(iii) Ignoring the motion of E between t'_1 and t_1, we have

$$z_1 - z'_1 = -\epsilon. \tag{7}$$

The delay is therefore given by

$$\begin{aligned} \Delta_{\rm r}(\lambda_a) &= t_1 - t_0 + \frac{z_1 - z_0}{c} \\ &= \frac{r_{\rm AB}(\lambda_a) - \epsilon}{c}(1 - \sin\lambda_a \sin i) + P'_{\rm A}\frac{\theta}{2\pi} + O\left(\epsilon c^{-2}\right), \end{aligned} \tag{8}$$

where the subscript 'r' indicates that we are taking into account the Rømer delay only. In this equation, we use $P'_{\rm A} = P_{\rm A}(1 + v_{l,A}/c)$ to represent the spin period of A with the classical Doppler correction due to its orbital velocity. This equation is valid at the SSB if we use the orbital parameters as measured there.

In Appendix A, we present a detailed calculation of the relativistic contribution to the total response delay Δ, known as the 'Shapiro delay' ($\Delta_{\rm s}$). For the range of orbital phases where we observe B's responses $\Delta_{\rm s}$ changes 4 μs, i.e. smaller than the rms timing precision of A. We can therefore assume $\Delta = \Delta_{\rm r} + \Delta_{\rm s} \simeq \Delta_{\rm r}$ for the remainder of this paper.

2.3 Distance between A at transmission and B at response

Having calculated the response delay as a function of λ_a and the separation between the two pulsars, $r_{\rm AB}(\lambda_a)$, we now calculate these two quantities as a function of $\lambda_{\rm A}$ at t'_0. The reason for this is that $\lambda_{\rm A}$ can be calculated precisely for any given time using the equations in Damour & Deruelle (1985, 1986); furthermore, this quantity determines the instantaneous configuration of the system.

In the equations that follow, we will only use the Newtonian terms to $O(c^{-2})$. A detailed calculation shows that the $O(c^{-3})$ Newtonian terms are much smaller than the rms timing precision of A. This means that they can be ignored for our present purposes.

At t'_0, the separation of pulsar I (A or B) from the centre of mass is given (see e.g. Roy 1988) by

$$d_{\rm I} = a_{\rm I}\frac{1 - e^2}{1 + e\cos f}, \tag{9}$$

where $a_{\rm I}$ is the semimajor axis of its orbit, e is the orbital eccentricity and the angle f is the true anomaly of the system at t'_0 ($f = \lambda_{\rm I} - \omega_{\rm I}$, where $\omega_{\rm I}$ is the longitude of periastron of pulsar I at t'_0). The components of a pulsar's velocity along the radial (i.e. away from the centre of mass) and transverse directions are given (Roy 1988) by

$$\dot{d}_{\rm I} = v_{\rm I} e \sin f, \tag{10}$$

$$d_{\rm I}\dot{f} = v_{\rm I}(1 + e\cos f), \tag{11}$$

where

$$v_{\rm I} = \frac{2\pi}{P_{\rm b}}\frac{a_{\rm I}}{\sqrt{1 - e^2}}, \tag{12}$$

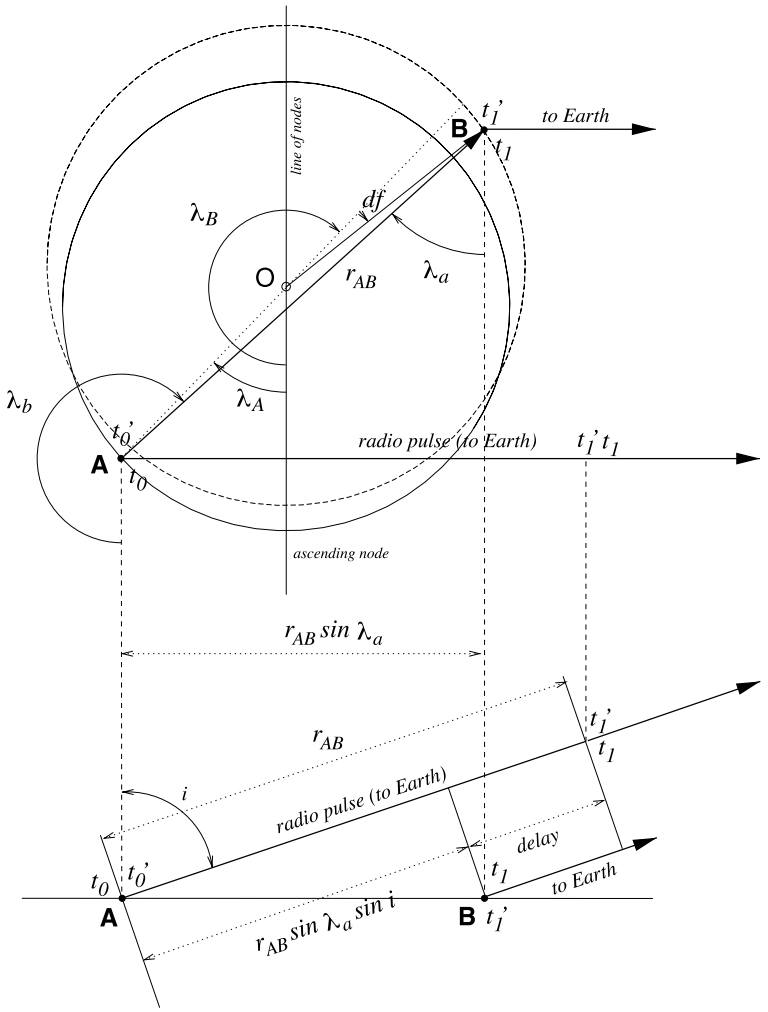

Figure 2. Emission (at t_0', on A) and reception at the position of B (at t_1') of the EM signal that causes B's responses. Upper diagram: events depicted in the orbital plane. O represents the centre of mass of the system, orbital motion is represented as clockwise. Lower diagram: events depicted on a plane that is perpendicular to the orbital plane and the plane of the sky. This contains the line-of-sight to the Earth and allows a representation of the response delays. The orbital inclination i of the PSR J0737−3039 binary system is much closer to 90° than depicted in this figure (Kramer et al. 2006); we represent it as being substantially lower for clarity. The difference in the locations of t_0, t_0' and t_1', t_1 is too small to be discerned at this scale. In this figure, the line of periastron just happens to coincide with the line of nodes, with $\omega_A = 180°, \omega_B = 0°$.

is the transverse velocity of pulsar I at quadrature ($f = \pi/2$) and P_b is the orbital period of the binary. The velocity of that pulsar relative to Earth is given by (e.g. Green 1985)

$$v_{l,I} = v_I \sin i\,(\cos\lambda_I + e\cos\omega_I)\,. \tag{13}$$

Calculating this velocity for A, we can immediately quantify the Doppler correction term for P_A in equation (8).

To calculate the instantaneous distance between the pulsars (d_{AB}), we replace a_I by $a = a_A + a_B$ in equation (9). During the time it takes A's signal to cross this distance (d_{AB}/c), B is moving. Because the EM signal is moving in the radial direction, only the radial component of B's motion (dr) will affect the travel time between the two pulsars. During the cross time $dr \simeq \dot{d}_B d_{AB}/c$, i.e. the distance between the events at t_0' and t_1' is

$$r_{AB}(\lambda_A) = d_{AB} + dr = d_{AB}\left(1 + \frac{v_B}{c} e \sin f\right) + O\left(c^{-2}\right); \tag{14}$$

the perpendicular motion of B between t_0' and t_1' is

$$dr_\perp \equiv d_B df = d_B \dot{f}(t_1' - t_0') = v_B(1 + e\cos f)\frac{r_{AB}(\lambda_A)}{c}. \tag{15}$$

Looking at Fig. 3, we can see that

$$\lambda_a = \lambda_A + \frac{dr_\perp}{r_{AB}(\lambda_A)} = \lambda_A + \frac{v_B}{c}(1 + e\cos f). \tag{16}$$

In the derivation above, we made the approximation that λ_a is the longitude of A as seen from B at t_1'. The longitude of A as seen from point E at t_1 is larger by a very small amount, $\epsilon \sin i \cos\lambda_a / r_{AB}$.

Noting that $dx = dr_\perp \cos\lambda_A$,

$$r_{AB}(\lambda_A)\sin\lambda_a = r_{AB}(\lambda_A)\sin\lambda_A + dr_\perp \cos\lambda_A. \tag{17}$$

With this result, we can rewrite equation (8) as a function of λ_A:

$$\Delta(\lambda_A) = \frac{r_{AB}(\lambda_A) - \epsilon}{c}(1 - \sin\lambda_A \sin i) - \frac{dr_\perp}{c}\cos\lambda_A \sin i + P_A' \frac{\theta}{2\pi} + O(\epsilon c^{-2}). \tag{18}$$

Using equations (9), (14) and (15), we can rewrite this as a function of a Keplerian term, $K(\lambda_A)$, which can be calculated from known orbital parameters and the system's geometry, and the unknown

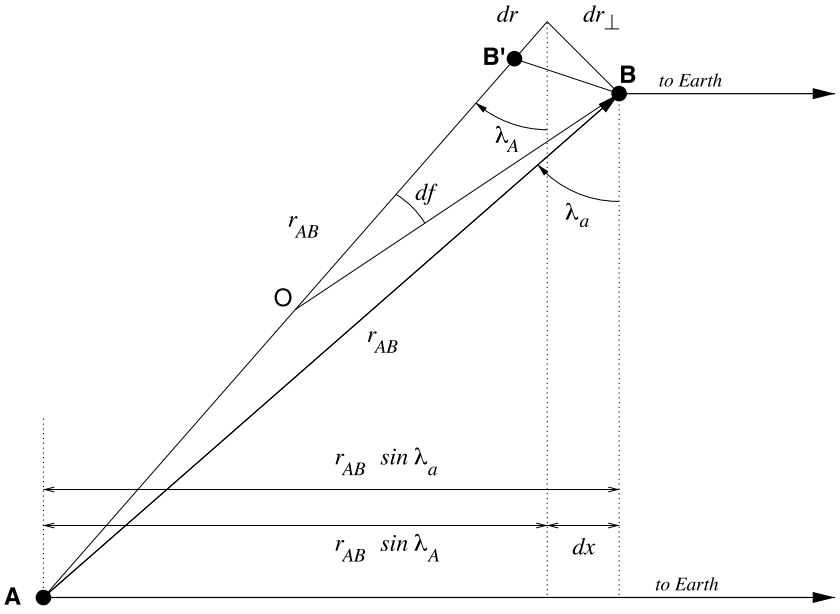

Figure 3. Detail on the motion of B in the orbital plane of the system. O represents the centre of mass of the system.

quantities ϵ and θ:

$$\Delta(\lambda_{\rm A}) = K(\lambda_{\rm A}) - \frac{\epsilon}{c}\left(1 - \sin\lambda_{\rm A}\sin i\right) + P'_{\rm A}\frac{\theta}{2\pi} + O(\epsilon c^{-2}) \quad (19)$$

$$K(\lambda_{\rm A}) = \frac{a}{c}\left(1-e^2\right)\left[\frac{1-\sin\lambda_{\rm A}\sin i}{1+e\cos f}\left(1+\frac{v_{\rm B}}{c}e\sin f\right) - \frac{v_{\rm B}}{c}\cos\lambda_{\rm A}\sin i\right] + O\left(c^{-3}\right). \quad (20)$$

The $K(\lambda_{\rm A})$ term is the time difference, measured at the SSB, between the events that occurred at t'_1 and t'_0 in the reference frame of the binary; it is by far the largest contribution to the response delay.

3 COMPARING MEASUREMENTS OF RESPONSE DELAYS WITH PREDICTIONS

So far, we have just made a theoretical calculation of the response delays, $\Delta(\lambda_{\rm A})$. We now discuss what we can learn from actually measuring such delays.

3.1 Measuring absolute delays

If we measure $\Delta(\lambda_{\rm A})$ for several $\lambda_{\rm A}$ in a single orbit and subtract $K(\lambda_{\rm A})$, we can measure the delays that are not a priori predictable:

$$\Delta(\lambda_{\rm A}) - K(\lambda_{\rm A}) = \frac{\epsilon}{c}\left(\sin\lambda_a\sin i - 1\right) \pm P'_{\rm A}\left(\frac{\lambda_a}{2\pi} - \frac{\phi_e}{2\pi} - \frac{1}{4}\right). \quad (21)$$

In order to measure $\Delta(\lambda_{\rm A})$, we have to specify a particular radio pulse of A (in principle, the closest to the time of emission of the EM signal that caused that particular response) and subtract its (barycentric) time from the response's barycentric time. However, because we have no prior knowledge of the terms in equation (21), there is some ambiguity in the choice of the pulse that is closest to that time of emission.

An experimental method that does away with the issue of the choice of a pulse of A and even the measurement of $\Delta(\lambda_{\rm A})$ entirely would proceed along the following lines.

(i) B's responses are particularly noticeable in an intensity grey-scale plot of time versus spin phase of B as presented by McLaughlin et al. (2004). In such a plot, we can determine the precise spin phase corresponding to each response; the precise method to accomplish this and the attainable precision will be discussed elsewhere.

(ii) In the next step, we convert this phase into a barycentric time. This can be achieved using the software package TEMPO.[3] The result corresponds to an event that occurred at t_1 in the reference frame of the binary.

(iii) Subtracting $K(\lambda_{\rm A})$, we obtain a second barycentric time that nearly corresponds to A's emission of the EM pulse [$(t'_0 + \epsilon/c \sin\lambda_{\rm A}\sin i$) in the reference frame of the binary]. At this time, we calculate $\lambda_{\rm A}$ from the binary's ephemeris.

(iv) Subtract the nearest time at which the rotational phase of A is zero. This time should be the equivalent of $\Delta(\lambda_{\rm A}) - K(\lambda_{\rm A})$. By fitting this to equation (21), we should be able to determine ϵ, ϕ_e and the direction of the spin of A.

With data from different orbits, we can also get a sense for the stability of ϕ_e and ϵ. Thus far, we have assumed that ϵ (the height above B where the response is produced) is a constant as a function of B's rotational phase. It is possible, however, that ϵ varies with B's spin phase. This would also introduce a secular variation of the ϵ observed for any spin phase of B due to the pulsar's geodetic precession. If that is the case, we could map the height of E above B as a function of the precession phase. Confusion with $K(\lambda_{\rm A})$ can be avoided because, despite the fact that both terms vary with $1 - \sin\lambda_{\rm A}\sin i$, only the latter varies with $(1 + e\cos f)^{-1}$.

[3] http://www.atnf.csiro.au/research/pulsar/tempo/

3.2 Delay variations at a constant λ_A

The response delays $\Delta(\lambda_A)$ will vary in time for any given λ_A because of the apsidal motion $\dot{\omega}$ changes f, which causes a change in $K(\lambda_A)$:

$$\delta_{t_2-t_1}(\lambda_A) \equiv \Delta_{t=t_2}(\lambda_A) - \Delta_{t=t_1}(\lambda_A) = \frac{a}{c}\left(1-e^2\right)(1-\sin\lambda_A \sin i)\,[j\,(t_2) - j\,(t_1)], \quad (22)$$

where t_1 and t_2 are two epochs at which the longitude λ_A occurs and

$$j(t) = \left(1 + \frac{v_B}{c} e \sin f\right)(1 + e\cos f)^{-1}. \quad (23)$$

Other terms of order larger than c^{-3} cancel out in the subtraction because of the constant λ_a, and the same happens for the terms dependent on θ and ϵ.[4] The variation of the Doppler correction to P_A are <1 μs and can therefore be ignored.

The $\delta_{t_2-t_1}(\lambda_A)$ are important because, being due solely to a variation of $K(\lambda_A)$, they are proportional to a. The maximum variation occurs between the time when λ_A coincides with periastron ($f = 0$, occurring at $t = t_p$) and apastron ($f = \pi$, occurring at $t = t_a$, which for PSR J0737−3039 is about 10.65 yr later):

$$\delta_{t_a-t_p}(\lambda_A) = \frac{2ae}{c}(1 - \sin\lambda_A \sin i). \quad (24)$$

In a single 2003 observation, McLaughlin et al. (2004) observe B's responses from $\sim 195^\circ < \lambda_B < \sim 225^\circ$, i.e. occurring shortly before the magnetosphere of B eclipses A at $\lambda_B = 270^\circ$. This corresponds to $\sim 15^\circ < \lambda_A < \sim 45^\circ$. At these extremes, we have $\delta_{t_a-t_p}(\lambda_A) = 0.3814(3)$ s and $0.1508(1)$ s. The uncertainty in this prediction is entirely due to the uncertainty of a (which results entirely from the uncertainty in the measurement of a_B); it represents 0.5–1.5 per cent of a rotation of A; this means that we should be able to keep track of the response delays with very high confidence.

The variations themselves are certainly measurable, since they are equivalent to many rotations of A. This means that we can always make an independent measurement of a. Depending on the precision and number of measurements of $\Delta(\lambda_A)$, the value of a derived in this fashion might be more precise than the present value derived from timing. In that case, we can improve our knowledge of the mass ratio:

$$R = \frac{a \sin i}{c x_A} - 1, \quad (25)$$

where x_A is the projected semimajor axis of A's orbit, in light seconds; this quantity is directly and very precisely measured from the timing of A. This equation (and also equations 22 and 24) show that, to determine R from a and x_A we need to know $\sin i$. We could in principle determine $\sin i$ independently from comparing measurements of $\delta_{t_2-t_1}(\lambda_A)$ made at different orbital longitudes. However, most theories of gravitation predict the Shapiro 's' term to be the same as $\sin i$ (Damour & Taylor 1992; Will 1993); therefore such an independent determination is not likely to be a useful test of gravitation. For this reason, we can use the extremely precise estimate of $\sin i$ from s in the estimate of R.

Finally, we remark that there is a small difference between the intrinsic and observed semimajor axes of the pulsar's orbits that is caused by aberration effects. Kramer et al. (2006) estimate that for A these are of the order of $10^{-6} x_A$, i.e. about 1 μs; this is similar to the level of precision for the measurement of x_A. It is highly unlikely that we will measure a to a similar precision, so this should not be a problem for the determination of R in equation (25). For B, Kramer et al. estimate that the effect of aberration should be of the order of $10^{-4} x_B$. It might be possible that we measure $x_B = a \sin i/c - x_A$ to better than the necessary level of precision. However, to be able to measure the aberration directly, we must be able to measure x_B from timing with this level of accuracy, so that the difference between the two values becomes evident. The intrinsic uncertainty of the x_B obtained from timing is about 10^{-3} x_B (Kramer et al. 2006), one order of magnitude larger than the effect of aberration. Therefore, unless the direct timing of B improves by more than one order of magnitude, the effects of aberration will not be separately measurable.

[4] The latter term is likely to cancel even if the main assumption in Section 2.1 is not correct, i.e. it only requires that any terms dependent on ϵ vary with λ_a in a repeatable way.

4 IMPLICATIONS AND PROSPECTS

In this paper, we have calculated the delay between the radio pulses of A and the modulated radio pulses of B, $\Delta(\lambda_A)$, assuming a simple scenario for that modulation, i.e. that it happens at the point, E, where the radio emission of B is being produced and that the modulating signal is travelling from A to E at the speed of light. Things could be more complicated, particularly considering that this trajectory must intersect the magnetosphere of B.

We will present details of the measurements of $\Delta(\lambda_A)$ and their timing analysis elsewhere. If the response delays obey the equations presented above in a consistent manner, that will validate our model. In that case, the measurement of these delays relative to the radio pulses of A will provide new and important astrophysical results.

First, a determination of the sense of A's rotation relative to its orbit, something never achieved for any other pulsar, would introduce fundamental constraints on binary evolution scenarios for this pulsar, as well as improved constraints on B's supernova kick. Finding that the orbital angular momentum is anti-aligned with A's angular momentum would require a very large supernova kick (Bailes 1988). Previous studies (e.g. Stairs et al. 2006; Willems et al. 2006) predict instead that the kick that produced B was rather small, therefore the angular momenta should be aligned. A confirmation of this alignment, combined with the small angle between the momenta, would introduce stringent constraints on the magnitude of the kick. Furthermore, we would know the sign of the expected relativistic spin-orbit contribution to $\dot{\omega}$ (Damour & Schäfer 1988). It is probable that this contribution will be measured in the near future (Kramer & Wex 2009); that would allow an estimate of A's moment of inertia. The moment of inertia of A, together with the well-determined mass of the pulsar, will introduce fundamental constraints on the equation of state for dense matter (Lattimer & Schutz 2005).

Secondly, by measuring ϵ, or by introducing upper limits to it, we might be able to locate the region where the EM signal from A is modulating the radio signal from B and relate it to the region where we expect the radio emission of B is being generated. Thus far, the best location of pulsar radio emission comes from the interpretation of multifrequency polarimetric pulse profiles in light of a relativistic version of the familiar rotating vector model (Blaskiewicz et al. 1991); the results indicate an emission height of a few hundred km. If the signal is being modulated as it is being generated, then ϵ should be of the order of a few ms and therefore a measurable quantity. If ϵ is significantly larger, then the modulation is happening after B's radio signal is generated.

Thirdly, we will make an independent measurement of the orbital separation of the two pulsars, a. If the timing of B's responses is precise enough, this might give us a more precise measurement of

the mass ratio of A and B, which would increase the precision of some of the previous tests of general relativity carried out in this binary system. This is a key input parameter for the general tests on conservative gravity theories outlined in Kramer & Wex (2009).

In the ideal case that we can track the response times well, one might think of their reception at the Earth as being equivalent to having a radio telescope at an altitude ϵ above B tracking A's rotation and then relaying the results live to Earth. This analogy highlights how fortunate we are to have a phenomenon like B's responses.

ACKNOWLEDGMENTS

PCCF, DRL and MAM acknowledge support from a WVEPSCoR research challenge grant held by the WVU Center for Astrophysics. MAM is an Alfred P. Sloan Fellow. Pulsar research at UBC is supported by an NSERC Discovery Grant. IHS acknowledges sabbatical support from the ATNF Distinguished Visitor program.

REFERENCES

Bailes M., 1988, A&A, 202, 109
Blaskiewicz M., Cordes J. M., Wasserman I., 1991, ApJ, 370, 643
Breton R. P. et al., 2008, Sci, 321, 104
Brumberg V. A., 1991, Essential Relativistic Celestial Mechanics. Adam Hilger, Bristol and New York
Burgay M. et al., 2003, Nat, 426, 531
Burgay M. et al., 2005, ApJ, 624, L113
Damour T., Deruelle N., 1985, Ann. Inst. Henri Poincaré, 43, 107
Damour T., Deruelle N., 1986, Ann. Inst. Henri Poincaré, 44, 263
Damour T., Schäfer G., 1988, Nuovo Cimento, 101, 127
Damour T., Taylor J. H., 1992, Phys. Rev. D, 45, 1840
Ferdman R., 2008, PhD thesis, Univ. British Columbia
Green R. M., 1985, Spherical Astronomy, Cambridge Univ. Press, Cambridge and New York
Kramer M., Stairs I. H., 2008, ARA&A, 46, 541
Kramer M., Wex N., 2009, Class. Quantum Gravity, 26(7), 073001
Kramer M. et al., 2006, Sci, 314, 97
Lattimer J. M., Schutz B. F., 2005, ApJ, 629, 979
Lorimer D., Kramer M., 2005, Handbook of Pulsar Astronomy, Cambridge Univ. Press, Cambridge
Lyne A. G. et al., 2004, Sci, 303, 1153
Manchester R. N. et al., 2005, ApJ, 621, L49
McLaughlin M. A. et al., 2004, ApJ, 613, L57
Roy A. E., 1988, Orbital Motion, Institute of Physics Publishing, Bristol and Philadelphia
Stairs I. H., Thorsett S. E., Dewey R. J., Kramer M., McPhee C. A., 2006, MNRAS, 373, L50
Will C. M., 1993, Theory and Experiment in Gravitational Physics. Cambridge Univ. Press, Cambridge
Willems B., Kaplan J., Fragos T., Kalogera V., Belczynski K., 2006, Phys. Rev. D., 74, 043003

APPENDIX A

Including post-Newtonian corrections, the time taken for a photon to propagate from the point of emission $\boldsymbol{x}_0$ to $\boldsymbol{x}$ in the gravitational field of an N-body system is given by

$$t - t_0 = \frac{|\boldsymbol{x} - \boldsymbol{x}_0|}{c} + \frac{2G}{c^3}\sum_{i=1}^{N} m_i \ln\left[\frac{r_{0i} + r_i + R}{r_{0i} + r_i - R}\right], \quad \text{(A1)}$$

where m_i is the mass of the ith body located at $\boldsymbol{x}_i$, $r_{0i} \equiv |\boldsymbol{x}_i - \boldsymbol{x}_0|$, $r_i \equiv |\boldsymbol{x} - \boldsymbol{x}_i|$ and $R \equiv |\boldsymbol{x} - \boldsymbol{x}_0|$ (Brumberg 1991). The first term, $|\boldsymbol{x} - \boldsymbol{x}_0|/c$, is the Rømer term used in the main text. The second term, the relativistic correction, is the sum of the Shapiro delays caused by the individual bodies in the N-body system.

We now apply equation (A1) to the signal propagation discussed in this paper (see Figs 1 and 2). Neglecting terms smaller than a few μs one finds for the signal propagating from A to Earth at distance D

$$\Delta_s^{(\mathrm{A}\oplus)} \simeq \frac{2Gm_\mathrm{A}}{c^3}\ln\left[\frac{D}{\delta_\mathrm{R}}\right] + \frac{2Gm_\mathrm{B}}{c^3}\ln\left[\frac{2D}{d_\mathrm{AB}(1+\cos\lambda_{a,\oplus})}\right]. \quad \text{(A2)}$$

$\delta_\mathrm{R}(\ll d_\mathrm{AB})$ is the emission height of the radio signal in the magnetosphere of A and $\lambda_{a,\oplus}$ is the angle between the direction to Earth and the direction to pulsar A as seen from B. For the signal propagating from A to the point E to sufficient accuracy

$$\Delta_s^{(\mathrm{AE})} \simeq \frac{2Gm_\mathrm{A}}{c^3}\ln\left[\frac{d_\mathrm{AB}}{\delta_\mathrm{EM}}\right] + \frac{2Gm_\mathrm{B}}{c^3}\ln\left[\frac{2d_\mathrm{AB}}{\epsilon(1+\cos\lambda_{a,\oplus})}\right]. \quad \text{(A3)}$$

$\delta_\mathrm{EM}(\ll d_\mathrm{AB})$ is the emission height of the EM signal that triggers the subpulse emission at E. Finally, for the subpulse signal emitted at E the Shapiro delay is given by

$$\Delta_s^{(\mathrm{E}\oplus)} \simeq \frac{2Gm_\mathrm{A}}{c^3}\ln\left[\frac{2D}{d_\mathrm{AB}(1-\cos\lambda_{a,\oplus})}\right] + \frac{2Gm_\mathrm{B}}{c^3}\ln\left[\frac{D}{\epsilon}\right]. \quad \text{(A4)}$$

The contribution of the Shapiro delays to Δ is therefore given by

$$\begin{aligned}\Delta_\mathrm{s} &= \Delta_\mathrm{s}^{(\mathrm{AE})} + \Delta_\mathrm{s}^{(\mathrm{E}\oplus)} - \Delta_\mathrm{s}^{(\mathrm{A}\oplus)} \\ &= \frac{2Gm_\mathrm{A}}{c^3}\ln\left[\frac{2}{1+\sin i\,\sin\lambda_\mathrm{A}}\right] + \frac{2Gm_\mathrm{A}}{c^3}\ln\left[\frac{\delta_\mathrm{R}}{\delta_\mathrm{EM}}\right] \\ &\quad + \frac{4Gm_\mathrm{B}}{c^3}\ln\left[\frac{d_\mathrm{AB}}{\epsilon}\right], \end{aligned} \quad \text{(A5)}$$

where we have used $\cos\lambda_{a,\oplus} = -\sin i\,\sin\lambda_\mathrm{A}$. The second term of equation (A5) is constant and, to sufficient accuracy, can be absorbed in ϕ_e. The third term of equation (A5) changes along the eccentric orbit with an amplitude of just 2 μs, and therefore can be absorbed into ϕ_e as well. In principle, the first term of equation (A5) can change quite significantly along the orbit, as $\sin i \simeq 1$ in the double pulsar (Kramer et al. 2006). However, as mentioned above, the subpulses are only observed in the range $\sim 15^\circ < \lambda_\mathrm{A} < \sim 45^\circ$. Across this interval, the first term of equation (A5) changes by less than 4 μs. Consequently, Shapiro delays can be ignored in the calculations of this paper.

This paper has been typeset from a TEX/LATEX file prepared by the author.